Renewable Energy 232 (2024) 121023

Contents lists available at ScienceDirect

Renewable Energy

journal homepage: www.elsevier.com/locate/renene

Theoretical models for predicting ventilation performance of vertical solar chimneys in tunnels

Youbo Huang [a,b], Bing Wang [a], Chengjia Luo [a], Long Shi [b,*], Ning Lu [a], Bingyan Dong [a], Hua Zhong [c,**]

[a] College of Safety Engineering, Chongqing University of Science and Technology, Chongqing, China
[b] State Key Laboratory of Fire Science, University of Science and Technology of China, Hefei, Anhui 230026, China
[c] School of the Built Environment and Architecture, London South Bank University, London, SE1 0AA, United Kingdom

ARTICLE INFO

Keywords:
Solar chimney
Urban tunnel
Natural ventilation
Renewable energy
Energy efficiency
Three-dimensional temperature distribution
Analytical model

ABSTRACT

Solar chimney as a reliable renewable energy system has been primarily utilized for building ventilation, but its application in the tunnel is rarely explored. This study develops theoretical models to predict the ventilation performance of vertical solar chimney in urban tunnel. Five temperature distribution types within the chimney cavity are analyzed, including uniform, vertically linear, horizontally semi-parabolic, two piecewise semi-parabolic in the depth direction, and three-dimensional parabolic profiles. The theoretical models consider the effect of chimney configuration, tunnel geometry, glazing materials, and solar radiation intensity on airflow rate through solar chimney. Validation against experimental data and numerical simulation shows that considering three-dimensional temperature distributions results in an average 11 % deviation from validation data, outperforming assumptions of uniform (29.3 % deviation) or lower-dimensional profiles. The volumetric flow rate through solar chimney exponentially decreased with h/w and h/d that the optimum ratio of h/d is 10. The airflow rate linearly increased with 0.14 power of glazing absorptivity. This analysis provides technical guidance for optimizing solar chimney design in tunnels, enhancing natural ventilation, and reducing energy consumption for mechanical ventilation systems.

Nomenclature

A	cross-section area of orifice (m^2)
A_c	cross section area of the chimney cavity (m^2)
A_t	cross-section area of tunnel (m^2)
A^*	area coefficient
B	buoyancy force (m^4/s^3)
C_d	coefficient of discharge
c_p	specific heat capacity (J/(kg. K))
D_c	hydraulic diameter of cavity (m)
D_t	hydraulic diameter of tunnel (m)
d	cavity depth (m)
d_{aw}	distance from absorber to lowest temperature position (m)
E	power of heating source (kW)
E_{aw}	absorbed solar energy by absorber (kW)
E_{gw}	absorbed solar energy by glazing (kW)
g	acceleration of gravity (m/s^2)
h	cavity height (m)
L_t	tunnel length (m)

(*continued on next column*)

(*continued*)

$\triangle P$	pressure difference (Pa)
$\triangle P_\zeta$	local resistance (Pa)
$\triangle P_\lambda$	friction resistance (Pa)
q_{sol}	solar radiation intensity (kW/m^2)
T_0	ambient temperature (K)
T_{aw}	temperature near absorber (K)
T_c	cavity temperature (K)
T_d	maximum temperature (K)
T_{dw}	maximum temperature near absorber (K)
T_{gw}	temperature near glazing (K)
T_s	transversely temperature (K)
T_{sw}	maximum temperature at sidewall surface (K)
T_x	temperature along the depth direction (K)
u	velocity (m/s)
u_t,	airflow velocity inside tunnel (m/s)
u_{in}	airflow velocity at the inlet (m/s)
u_{out}	airflow velocity at the outlet (m/s)
V	volumetric flow rate (m^3/s)

(*continued on next page*)

* Corresponding author.
** Corresponding author.
E-mail addresses: shilong@ustc.edu.cn (L. Shi), hua.zhong@ntu.ac.uk (H. Zhong).

https://doi.org/10.1016/j.renene.2024.121023
Received 12 November 2023; Received in revised form 23 June 2024; Accepted 16 July 2024
Available online 17 July 2024

(*continued*)

V_{in}	volumetric flow rate for uniform temperature (m^3/s)
V'_{in}	volumetric flow rate for vertically linear temperature (m^3/s)
V''_{in}	volumetric flow rate for semi-parabolic temperature (m^3/s)
$V''_{in,ls}$	volumetric flow rate both considering vertically linear and horizontally semi-parabolic temperature (m^3/s)
$V'''_{in,lts}$	volumetric flow rate both considering vertically linear and two piecewise parabolic temperature (m^3/s)
$V'''_{in,ltw}$	volumetric flow rate considering three-dimensional temperature (m^3/s)
w	cavity width (m)
x, y	coordinate (m)
Greek letters	
δ	absorptivity of absorption wall
ε	absorptivity of glazing wall
ζ_{en}	local resistance coefficient of entry
ζ_{in}	local resistance coefficient at inlet
ζ_{out}	local resistance coefficient at outlet
ρ_0	ambient density (kg/m^3)
ρ_c	air density inside channel (kg/m^3)
τ	transmissivity of glazing
Π	velocity coefficient

1. Introduction

The energy consumption in buildings contributes to over 40 % of the total energy consumed [1,2]. Heating, ventilation, and air conditioning, as the largest consumers, account for 20 % of the world's total energy usage [3]. The overuse of traditional energy sources (fossil fuel) accelerates not only the energy crisis but also climate change. Therefore, renewable energy has been focused on much attention as a release from the current crisis. Solar chimney is one of the basic renewable energy systems. The solar chimney consists of a channel cavity (constructed by an absorption wall and a glazing wall) and inlet/outlet openings. The internal air inside the channel cavity is heated by solar radiation that penetrates through the glazing wall. Thus, a temperature gradient is occurred between inlet and outlet, which results in an air density difference due to the ideal gas law. The airflow inside the channel cavity is then driven by this thermal buoyancy. Recently, solar chimney has been extensively applied in building ventilation that can effectively reduce energy consumption and carbon emissions [4]. The annual consumption of fan shaft power could be reduced by approximately 50 % owing to the use of solar chimneys in building ventilation [5].

The ventilation performance of a solar chimney is always evaluated using the volumetric flow rate throughout the channel and its temperature rise. In recent years, four types of mathematical models have been proposed to predict the ventilation rate based on individual parameters, air temperature inside the cavity, density gradient, and solar radiation [6]. In fact, all these parameters relate to the incident solar radiation intensity that induces the air temperature gradient between the inlet and outlet. Numerous studies have been conducted to develop a theoretical model for solar chimneys. Ong [7] proposed a simple mathematical model to predict the ventilation performance of a solar chimney in a building using a thermal resistance network. Ong and Chow [8] conducted experiments to validate the accuracy of this model. They found that the temperature near the absorption wall is higher than that close to the glazing wall. Moreover, the theoretical model overestimated the mean temperature near the absorption wall under solar radiation of 670 W/m^2. Practically, the temperature gradient determines the air density difference inside the channel cavity that dominates the airflow velocity due to the stack effect. To accurately predict the airflow velocity, it is important to analyze the temperature distribution inside the channel cavity. Andersen [9] developed an analytical model for the natural ventilation rate of a solar chimney that considered the uniform air temperature distribution inside the channel. Shi [10] argued that this is the first comprehensive theoretical model for a wall solar chimney in a room with two openings (inlet and outlet). The previous model was mainly developed based on the uniform temperature rise between the inlet and outlet but ignored the transversal temperature distribution [6]. Nevertheless, under practical conditions, the temperature inside the solar chimney is not uniformly distributed. Shi and Zhang [11] found that the cavity height, area of window, and area of opening positively affected the airflow rate as the temperature distribution inside the solar chimney varied. Actually, the inside temperature increased with the channel height as more solar radiation was absorbed by the vertical wall to heat the inflow air. Thus, the assumption of uniform temperature is inappropriate because it overestimates the airflow rate by more than 26 % than the assumption of vertically linear temperature [12]. However, the air temperature close to the outlet decreases with the mixing of heated air and ambient air. From the experimental results, a quadratic equation is proposed, which correlates well with the vertical temperature inside the channel [8].

As solar radiation penetrates through the glazing wall and being absorbed by the collector, the temperature near the absorption wall is higher than the glazing wall temperature [5,13–15]. Cheng et al. [12] considered vertically linear and horizontally parabolic temperature distributions to establish an empirical model for solar chimney in tunnels under natural and fire conditions. However, the temperature profile in the cavity width direction has not been considered. Due to natural convection, the air temperature at cavity center may be lowest. The temperature distribution in the cavity width direction is like a parabolic curve, which is still not accounted for in the literature. Kong et al. [5] performed a two-dimensional (2D) computational algorithm to calculate the outflow rate through an inclined roof-top solar chimney by considering the temperature distribution in the depth direction. However, the air temperature in the width direction is not considered, and the mathematical model is not applicable to practical engineering as a complex input and calculated process. The realistic applications raise a great need for a universally applicable mathematical model that can account for the non-uniform temperature rise inside the channel, while the predictions could be closer to the actual situation.

Many realistic design factors influence the ventilation performance of solar chimney. There are four types of impact factors on the performance of solar chimneys: cavity configurations, installed configurations, material usages, and environmental conditions [6]. The ventilation performance is enhanced under possible high cavity and solar radiation, which has been accounted for in the analytical model developed by Shi et al. [11]. The ventilation rate is related to the 0.712 power of the cavity depth, which dominates the temperature difference in the horizontal depth direction [15]. Wang et al. [16] suggested that the cavity depth has an exponential effect on the airflow rate. The installed angle of the solar chimney influences both the stack height and total absorbed solar energy. Kong et al. [5] argued that the optimum inclination angle (varying from 45° to 60°) of a roof-top solar chimney depended on the latitude and season of operation, but they lacked an easy-to-use quantitative correlation. The use of phase change material, solar absorber with larger absorptivity and emissivity, and low-e coating could significantly improve the airflow through the chimney cavity [2,17]. Previous models for solar chimney performance were estimated based on one material usage but rarely quantified the influence of material usage. For environmental conditions, solar radiation, latitude [5], and external wind [18] are the main factors influencing the ventilation rate, which has attracted extensive attention. The incoming flow enhanced the natural ventilation rate; otherwise, the opposite wind reduced the ventilation performance [19]. Shi [20] proposed a theoretical model to account for the effect of wind on solar chimney performance in building ventilation. In total, the previous empirical models mainly consider the uniform inside temperature, vertically linear rising, and summit parabolic in depth direction. However, the temperature attenuation in the cavity width direction has not yet been considered, which may result in the separation of predicted values and practical data. The theoretical model for a solar chimney by considering the three-dimensional (3D) inside temperature is still lacking. Moreover, the previous model focused on the ground building, which is not applicable to underground space as a difference space structure.

An urban tunnel is a typical underground long-narrow confined space with two ends, which is different from a ground-room building with windows. Thus, the airflow behavior induced by thermal buoyancy could not be directly described using a recent analytical model based on room space. The study on solar chimneys in tunnels is limited. Cheng et al. [12] numerically studied the airflow velocity through a solar chimney in a tunnel and considered the symmetrical temperature profile between the glazing and absorption walls. Unfortunately, the glazing wall temperature is lower than the absorption wall temperature in a real building. Huang et al. [21] proposed two piecewise semi-parabolic function to correlate the temperature distribution along the cavity depth direction and correlated the volumetric flow rate through solar chimney in tunnel. However, the temperature distribution in the width direction as well as the influence of cavity width on airflow rate were also not considered in previous research. Practically, the rapid growth of traffic volume puts great pressure on the air quality in urban tunnel spaces. The shaft natural ventilation system and mechanical ventilation system are used to enhance the air quality. Only using the shaft is always with insufficient ventilation capacity; in contrast, the mechanical system can provide the required airflow velocity but is energy-consuming and costly [22]. The mechanical system in the Zhongnanshan Highway Tunnel in China consumes over 70 % of the total operational energy consumption [23]. Thus, the natural shaft is usually combined with a jet fan system to reduce energy use and maintain stable ventilation efficiency in urban underground spaces [24]. It is more effective for reducing the energy consumption and construction cost by employing the renewable energy ventilation system in tunnels, which contributes to relive energy crisis and carbon emission. A solar chimney applied to an urban tunnel can accelerate the airflow through the shaft as thermal buoyancy, thus improving the air change per hour in the tunnel. The appropriate cavity configuration of the solar chimney in the tunnel could achieve the ventilation requirement. However, there is a lack of theoretical support. The potential and limits of heating distribution on airflow are not fully understood. Therefore, it is urgent to deduce a universal theoretical model for the ventilation performance of solar chimneys in tunnels to promote the application of this zero-energy-consumption ventilation system in tunnels.

This study establishes a novel theoretical model for the volumetric flow rate through a solar chimney at the top of an urban tunnel. Influence of chimney configuration, tunnel configuration, material usage, and solar radiation intensity are all considered. The uniform temperature distribution inside the channel, vertically linear temperature, a semi-parabolic temperature distribution, two-pricewise parabolic temperature distributions in the cavity depth direction, and parabolic temperature in the cavity width direction (3D) are all analyzed. The previous numerical results and experimental data were carried out to validate the predictions. This study takes the knowledge of solar chimney performance in urban tunnels and in-depth explains the theory.

2. Mathematical models

A typical type of solar chimney in a tunnel is shown in Fig. 1, where the smokestack cavity is located at the top of the tunnel. The solar radiation penetrates the glazing wall and is absorbed by the absorption wall to heat the internal air inside the solar chimney cavity. The temperature gradient results in the density difference between the inlet and outlet of the channel cavity, which drives the airflow throughout the solar chimney. Meanwhile, fresh air enters the tunnel through two ends. The air temperature inside the channel cavity varies gradually in the three axis directions due to the different absorptivity and emissivity of the glazing wall and absorber, as well as the heat accumulation in the vertical direction. This temperature distribution affects the thermal buoyancy force that determines the airflow velocity through the solar chimney. Most previous models for solar chimneys assumed uniform temperature [9], vertically linear [10], and horizontally parabolic distribution in the depth direction [12] or even combined. The practical temperature near the absorber is higher than the glazing temperature, and the temperature rise close to the insulation sidewall is higher than the air temperature at channel center due to the heat convection transfer and radiation. In fact, the temperature in the depth direction is an asymmetric parabolic distribution, and the temperature in the cavity width direction is a symmetric parabolic variation that has not been accounted for in existing theoretical models [5,25,26]. In the following section, these typical types of temperature distribution, including uniform, vertically linear, semi-parabolic, and two piecewise semi-parabolic temperatures in the depth direction and parabolic temperature in the cavity width direction will be analyzed one by one to develop an analytical model for airflow velocity through the solar chimney in a tunnel.

2.1. Uniform temperature

The traditional model, which assumes well-mixed airflow and uniform temperature inside the chimney, for building solar chimney [9] and solar chimney in tunnel [12] was developed. However, the effect of tunnel configuration on airflow rate was not considered. This section establishes an analytical model for the ventilation rate of a solar chimney in a tunnel based on the uniform temperature distribution in the channel, while both the solar chimney and tunnel configurations are considered.

Fresh air enters the tunnel from two portals, and then air enters the solar chimney and flows out through the outlet of the channel. In this study, the following assumptions are made: (a) the airflow rate from the two portals of the tunnel is the same; (b) the interaction of two incident airflows from the tunnel to the cavity is ignored; (c) the hydrostatic pressure in the channel is considered linear with the cavity height; (d) the temperature rise inside the tunnel is neglected as minimal; (e) the area of the inlet and outlet is the same; (f) the discharge coefficients for all the orifices are considered the same [10]; and (g) this study focuses on predicting solar chimney performance under steady status. The airflow velocity is driven by thermal buoyancy (as temperature gradient) that resists the local resistance, friction resistance, and export kinetic energy. The local resistance includes the local resistance at the tunnel entry and the local resistance at the inlet and outlet, which is given by

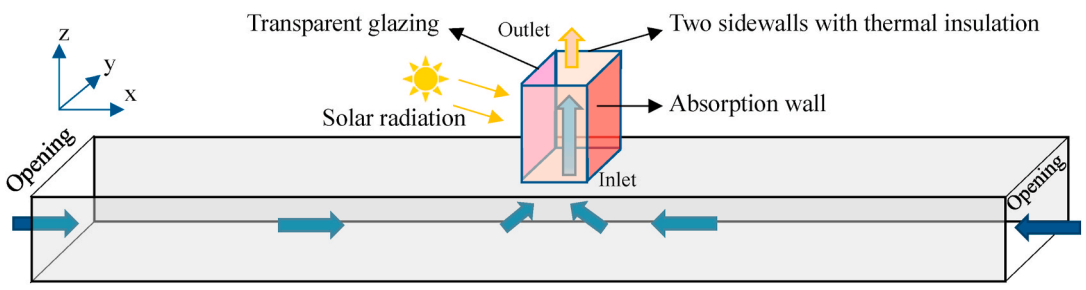

Fig. 1. Schematic of the solar chimney at the top of a tunnel.

$$\Delta P_\zeta = \frac{1}{2}\zeta_{en}\rho_0 u_t^2 + \frac{1}{2}\zeta_{in}\rho_0 u_{in}^2 + \frac{1}{2}\zeta_{out}\rho_c u_{out}^2 \quad (1)$$

The friction resistances exist both in the tunnel and solar chimney due to the surface roughness. The velocity at the outlet is used to calculate the friction resistance in the cavity, which is given by

$$\Delta P_\lambda = \frac{1}{2}\frac{L_t}{D_t}\rho_0 u_t^2 + \frac{1}{2}\frac{h}{D_c}\rho_c u_{out}^2 \quad (2)$$

The hydrostatic pressure difference depends on the air density gradient and the height difference between the inlet and outlet, which is given as

$$\Delta P = (\rho_0 - \rho_c)gh \quad (3)$$

Based on the relationship between hydrostatic pressure and dynamic pressure, the following equation is given as follows:

$$\Delta P_\zeta + \Delta P_\lambda = \Delta P \quad (4)$$

Under steady-state conditions, the following equation can be given based on the conservation of mass:

$$2\rho_0 A_t u_t = \rho_0 A_c u_{in} = \rho_{out} A_c u_{out} \quad (5)$$

Based on Eq. (4) and Eq. (5), the velocity at the inlet is given as

$$u_{in} = \sqrt{\frac{2(\rho_0 - \rho_c)gh}{\rho_0\left(\frac{A_c^2}{4A_t^2}\left(\zeta_{en} + \frac{L_t}{D_t}\right) + \frac{\rho_0}{\rho_c}\left(\zeta_{out} + \frac{h}{D_c}\right) + \zeta_{in}\right)}} \quad (6)$$

On the basis of the ideal gas law, the relationship between air density and temperature can be given with less than 0.02 % error [12]:

$$\rho_0 T_0 = \rho_c T_c \quad (7)$$

The volumetric flow rate through an orifice is given by

$$V = C_d A u \quad (8)$$

Based on Eqs. (6)–(8), the volumetric flow rate at the inlet is given as

$$V_{in} = C_d A_c \sqrt{\frac{2\rho_c(T_c - T_0)gh}{\rho_0\left(\frac{A_c^2}{4A_t^2}\left(\zeta_{en} + \frac{L_t}{D_t}\right) + \frac{\rho_0}{\rho_c}\left(\zeta_{out} + \frac{h}{D_c}\right) + \zeta_{in}\right)T_0}} \quad (9)$$

Usually, it is assumed that $\rho_0 = \rho_c$ in the denominator on the right-hand side of Eq. (9) [10]. The energy conservation equation for the chimney cavity under steady conditions is given as

$$E = \rho_c c_p V_{in}(T_c - T_0) \quad (10)$$

After combining the above equation, the volumetric flow rate at the inlet can be given as follows:

$$V_{in} = (C_d A^*)^{2/3}(2Bh)^{1/3} \quad (11)$$

$$A^* = \sqrt{\frac{4A_c^2 A_t^2}{A_c^2\left(\zeta_{en} + \frac{L_t}{D_t}\right) + 4A_t^2\left(\zeta_{out} + \frac{h}{D_c} + \zeta_{in}\right)}} \quad (12)$$

$$B = \frac{Eg}{\rho_0 c_p T_0} \quad (13)$$

2.2. Vertically linear temperature distribution

As solar radiation penetrates the glazing over the whole cavity height, the internal air is heated gradually from bottom to top due to convection heat transfer. Thus, the traditional model based on the uniform temperature distribution in the cavity is far from practical. The vertically linear temperature rise along the cavity height is more consist with actual program than uniform one. Cheng et al. [12] considered the vertically linear temperature to develop an empirical model for a solar chimney in a tunnel. However, the influence of tunnel dimension and resistance losses were not considered. Therefore, the advanced model is deduced considering both the vertically linear temperature distribution and tunnel configuration for completeness.

For the vertically linear temperature distribution, the temperature profile from the inlet to outlet increases linearly with cavity height $T_c = T_0 + kh$, k is the coefficient. Under natural ventilation conditions, the vertically linear density gradient can be obtained based on Eq. (7), where $\rho_c = \rho_0 - kh$. Therefore, the pressure difference in Eq. (3) between the inlet and outlet can be rewritten as

$$\Delta P = \int_0^h (\rho_0 - \rho_c)gdH = \frac{1}{2}(\rho_0 - \rho_{out})gh \quad (14)$$

The volumetric flow rate at the inlet of the solar chimney can be expressed as

$$V'_{in} = (C_d A^*)^{2/3}(Bh)^{1/3} \quad (15)$$

where V'_{in} is the volumetric flow rate considering the vertically linear temperature distribution.

The predicted volumetric flow rate by considering vertically linear temperature is equal to 79.4 % of the predictions by the traditional model; this relationship is consistent with previous study conducted by Cheng et al. [12].

$$\frac{V'_{in}}{V_{in}} = \sqrt[3]{\frac{1}{2}} = 0.794 \quad (16)$$

2.3. Horizontal semi-parabolic temperature

The uniform temperature distribution in the cavity depth direction is quite different from the actual situation mainly because of the convection heat transfer in the chimney cavity. The temperature rise near the glazing surface is lower than that over the absorption wall surface. Therefore, the semi-parabolic temperature distribution in the cavity depth direction is considered in this section to establish an analytical model for the ventilation rate through the solar chimney, as shown in Fig. 2(a) semi-parabolic.

Considering the semi-parabolic temperature distribution in the depth direction, the temperature attenuation from the glazing wall to the absorption wall can be given by

$$T_x = \frac{T_{dw} - T_0}{d^{3/2}}x^{3/2} + T_0 \quad (17)$$

Under these circumstances, the total absorbed solar energy can be given by

$$E = \int_0^d \kappa\left(\frac{T_d - T_0}{d^{3/2}}x^{3/2}\right)^{3/2} dx \ , \ \kappa = w\rho_0 c_p C_d\sqrt{\frac{gh}{T_0}} \quad (18)$$

Simplifying the above equation, the total energy with semi-parabolic temperature attenuation along the depth direction is given by

$$E = \frac{4}{13}\kappa(T_d - T_0)^{3/2}d \quad (19)$$

Based on the same total energy under uniform temperature distribution and semi-parabolic temperature distribution in the cavity depth direction, the following equation is given as

$$\frac{T_d - T_0}{T_c - T_0} = \frac{13^{2/3}}{4} \quad (20)$$

Substituting Eq. (20) into Eq. (9), then simplifying the equation, the model for ventilation rate is given as

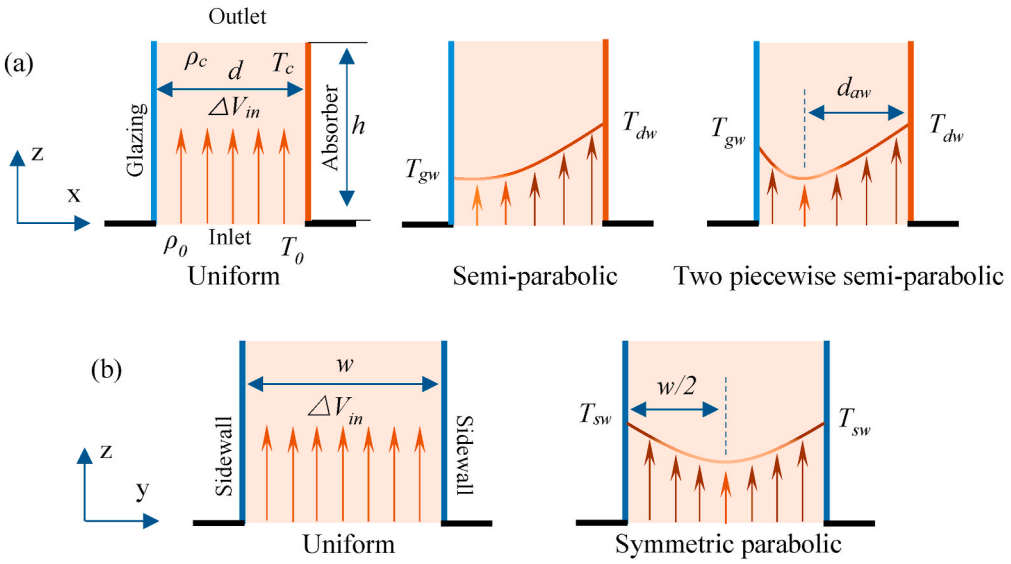

Fig. 2. Temperature distribution inside the channel: (a) in the depth direction and (b) in the width direction.

$$V_{in}^{''} = 0.928(C_d A^*)^{2/3}(2Bh)^{1/3} \tag{21}$$

where $V_{in}^{''}$ is the ventilation rate considering the semi-parabolic temperature in m^3/s, $V_{in}^{''} = 0.928\ V_{in}$. Considering both the vertically linear temperature and the horizontally semi-parabolic temperature distribution, the volumetric flow rate at the inlet is $0.737V_{in}$, expressed as

$$V_{in,ls}^{''} = 0.737(C_d A^*)^{2/3}(2Bh)^{1/3} \tag{22}$$

where $V_{in,ls}^{''}$ is the ventilation rate at the inlet considering both vertically linear temperature and horizontally semi-parabolic temperature distribution in m^3/s.

2.4. Two piecewise parabolic temperatures in the depth direction

Based on the experimental results [14] and numerical data [5], the inside temperature near the glazing is higher than the air temperature but lower than the absorption wall temperature. In practical conditions, away from the glazing and absorption walls, the temperature decays gradually because of convective heat transfer. Due to the continuous temperature distribution in the depth direction, the lowest temperature decay from the gazing wall and absorption wall is the same. Thus, two piecewise semi-parabolic temperatures with different peak values near the glazing and absorption wall can describe the horizontal temperature profile well, as shown in Fig. 2(a). Where the position of the lowest temperature along cavity depth is a key parameter that relates to the transmissivity and absorptivity of the glazing and absorber [21]. In this section, a theoretical analysis is provided to understand the temperature distribution in the depth direction. The position of the lowest temperature is determined. Moreover, an analytical model for this horizontally temperature distribution and volumetric flow rate is established.

The absorbed solar energy by the absorption wall is given by

$$E_{aw} = \delta\tau whq_{sol} \tag{23}$$

The total energy absorbed by the glazing wall is given by

$$E_{gw} = \varepsilon whq_{sol} \tag{24}$$

Based on Eq. (18), the total absorbed energy by the absorber and glazing can be obtained as

$$E_{aw} = \frac{4}{13}\kappa\left(\frac{T_{aw} - T_0}{d^{3/2}}\right)^{\frac{3}{2}}(d - d_{aw})^{13/4} \tag{25}$$

$$E_{gw} = \frac{4}{13}\kappa\left(\frac{T_{gw} - T_0}{d^{3/2}}\right)^{\frac{3}{2}} d_{aw}{}^{13/4} \tag{26}$$

From Eqs. (25) and (26), the temperature near the glazing and absorption wall can be respectively obtained as

$$T_{aw} = \left(\frac{13E_{aw}}{4\kappa(d - d_{aw})^{13/4}}\right)^{2/3} d^{3/2} + T_0 \tag{27}$$

$$T_{gw} = \left(\frac{13E_{gw}}{4\kappa d_{aw}{}^{13/4}}\right)^{2/3} d^{3/2} + T_0 \tag{28}$$

Substituting Eqs. (27) and (28) into Eq. (17), the temperature attenuation from two opposite walls in the depth direction can be predicted. Thus, the horizontal temperature in the depth direction is given by

$$\Delta T_x = \begin{cases} \left(\dfrac{13E_{gw}}{4\kappa d_{aw}^{13/4}}\right)^{2/3} x_0^{3/2}, 0 < x \le d_{aw} \\ \left(\dfrac{13E_{aw}}{4\kappa(d - d_{aw})^{13/4}}\right)^{2/3} x^{3/2}, d_{aw} < x < d \end{cases} \tag{29}$$

From Eq. (29), One unknown number of d_{aw} is deduced on the basis of the boundary condition that the lowest temperature from two sides is the same, expressed as

$$d_{aw} = \frac{d}{1 + \left(\frac{\delta\tau}{\varepsilon}\right)^{4/13}} \tag{30}$$

Under these circumstances, the volumetric flow rate at the inlet can be given as

$$V_{in}''' = C_d w \frac{A^*}{A_c}\left(\int_0^{d_{aw}} \sqrt{\frac{2gh(T_{gw} - T_o)x^{3/2}}{d^{3/2}T_0}}dx + \int_{d_{aw}}^{d} \sqrt{\frac{2gh(T_{aw} - T_o)x^{3/2}}{d^{3/2}T_0}}dx\right) \tag{31}$$

Integrating the above expression and simplifying, the volumetric flow rate at the inlet is given by

$$V_{in}''' = C_d w \frac{A^*}{A_c}\frac{4}{7}\sqrt{\frac{2gh}{d^{3/2}T_0}}\left(d_{aw}^{\frac{7}{4}}\Delta T_{gw}^{\frac{1}{2}} + \Delta T_{aw}^{\frac{1}{2}}\left(d^{\frac{7}{4}} - d_{aw}^{\frac{7}{4}}\right)\right) \tag{32}$$

Considering the vertically linear temperature distribution with a coefficient of 0.794, the volumetric flow rate at the inlet can be calculated as follows:

$$V'''_{in,lts} = 0.457 C_d \frac{A^*}{A_c} \Pi \tag{33}$$

$$\Pi = w\sqrt{\frac{2gh}{d^{3/2}T_0}}\left(d_{aw}^{\frac{7}{4}}\Delta T_{gw}^{\frac{1}{2}} + \Delta T_{aw}^{\frac{1}{2}}\left(d^{\frac{7}{4}} - d_{aw}^{\frac{7}{4}}\right)\right) \tag{34}$$

where $V'''_{in,lts}$ is the volumetric flow rate considering both linear vertical temperature and two piecewise parabolic temperature distributions in the depth direction in m^3/s, Π is the velocity coefficient.

2.5. Parabolic temperature distribution in the width direction

In order to fully utilizing the solar energy, two sides of the chimney cavity are covered by thermal insulation material. Thus, the transverse temperature in the cavity width direction decreases from the two sidewalls to channel center as convection heat transfer. Under these circumstances, the transverse temperature has a parabolic distribution that has not been studied in the literature. Fig. 2 (b) shows the transversely parabolic temperature distribution in the cavity width direction, which can be expressed as

$$T_s = \frac{4(T_{sw} - T_0)}{w^2}\left(y - \frac{w}{2}\right)^2 + T_0 \tag{35}$$

where T_{sw} is the maximum temperature at the sidewall surface in K, T_s is the transverse temperature in K, and y is the distance away from the sidewall in the cavity width direction.

The maximum temperature near the sidewalls can be predicted using the model for horizontal temperature along the cavity depth, Eq. (29). Therefore, the temperature distribution can be expressed as

$$\frac{\Delta T_s}{4} = \begin{cases} \dfrac{\left(\frac{13E_{gw}}{4\kappa d_{aw}^{13/4}}\right)^{2/3} x^{3/2}}{w^2}\left(y - \dfrac{w}{2}\right)^2, 0 < x < d_{aw} \\ \dfrac{\left(\frac{13E_{aw}}{4\kappa (d - d_{aw})^{13/4}}\right)^{2/3} x^{3/2}}{w^2}\left(y - \dfrac{w}{2}\right)^2, d_{aw} < x < d \end{cases} \tag{36}$$

The volumetric flow rate can be expressed as

$$V'''_{in\ ,\ ltw} = C_d \frac{A^*}{A_c} \int_0^w \int_0^d \sqrt{\frac{2gh(T_{\text{out}} - T_o)}{T_0}} dxdy \tag{37}$$

where $V'''_{in\ ,\ ltw}$ is the volumetric flow rate considering the vertically linear temperature distribution, horizontally two semi-parabolic temperature distributions, and transversely parabolic temperature distribution.

Integrated with the above equation and combined with Eq. (33), the volumetric flow rate considering the three-dimensional temperature distribution (3D) inside the chimney channel can be given as

$$V'''_{in.ltw} = \sqrt[3]{\frac{1}{2}} V'''_{in.lts} = 0.343 C_d \frac{A^*}{A_c} \Pi \tag{38}$$

3. Validation of the theoretical models

Table 1 presents a summary of analytical models for the volumetric flow rate through the solar chimney in the tunnel considering the five types of temperature distributions. if the vertically linear temperature distribution is considered, the volumetric flow rate is $0.794 V_{\text{in}}$ and drops 20.6 % compared with the traditional model. From the developed model, considering both the vertically linear and horizontally semi-parabolic temperature distribution in the depth direction, the volumetric flow rate is $0.737 V_{\text{in}}$. Thus, the predictions are less than 26.3 % of the traditional model. This reduced value is lower than 37 % of the previous model proposed by Cheng et al. [12], which considered both vertically linear and parabolic temperature distributions. Additionally, considering the transversely parabolic temperature distribution in the width direction, the volumetric flow rate drops 20.6 % compared to the predicted model considering vertically linear and horizontally two-parabolic temperature distributions.

The experimental results [21] and numerical data [12] for solar chimneys applied to tunnel ventilation is employed to validate the analytical model and compare the predictions under five types of temperature distributions. The experiments were conducted in a reduced scale tunnel with dimensions of 10 m (length) × 0.5 m (width) × 0.25 m (height). A solar chimney cavity with a width of 0.15 m and depth of 0.1m was installed at the top of the tunnel. The three cavity heights of 0.15m, 0.25 m, and 0.3m were considered. Three solar radiation intensities of 400 W/m^2, 600 W/m^2 and 800 W/m^2 were conducted in the experiments. The K-type thermocouples were used to measure the temperature with maximum measurement uncertainty less than 5 %. The airflow velocity was measured by hot-wire anemometer (KANOMAX model KA12) with maximum measurement uncertainty less than 7 %. A detailed description of the experiment can be found in Ref. [21]. The numerical modelling was briefly introduced, and more detail can be found in Ref. [12]. The dimensions of the tunnel are 100 m (length) × 7.6 m (width) × 4.8 m (height). The cavity depth of the solar chimney varied from 0.2 to 1.8 m. The cavity height increased from 1 m to 6 m with intervals of 1 m. The solar radiation intensity ranged from 200 W/m^2 to 1200 W/m^2 with intervals of 200 W/m^2. The discharge coefficient is 0.62 according to Fluid Mechanics [27]. A 3-mm-thick glazing with an absorptivity of 0.05 and transmissivity of 0.87 was considered. The absorptivity of the absorber was considered as 0.96.

Fig. 3 shows a comparison of the volumetric flow rate at the inlet. It can be observed that the predictions by the traditional model are higher than those by other types of models. The predictions of volume flow rate per hour under the five temperature distribution conditions are all higher than the experimental results. The predicted value using Eq. (38), which proposed based on 3D temperature profile, is close to the experimental data with an average deviation of 15.5 %. For comparison with full-scale numerical data, the traditional model overestimates the volumetric flow rate with an average deviation of 29.3 %. When considering the vertically linear temperature distribution, the average

Table 1
Analytical model for solar chimney in tunnel.

Temperature distribution	Analytical model	Note
Uniform Eq. (11)	$V_{in} = (C_d A^*)^{2/3}(2Bh)^{1/3}$	$A^* = \sqrt{\frac{4A_c^2A_t^2}{A_c^2\left(\zeta_{en} + \frac{L_t}{D_t}\right) + 4A_t^2\left(\zeta_{out} + \frac{h}{D_c} + \zeta_{in}\right)}}$
Vertically linear Eq. (15)	$V_{in} = (C_d A^*)^{2/3}(Bh)^{1/3}$	
Vertically linear, horizontally semi-parabolic Eq. (22)	$V'''_{in,ls} = 0.737(C_d A^*)^{2/3}(2Bh)^{1/3}$	
Vertically linear, horizontally two semi-parabolic Eq. (33)	$V'''_{in,lts} = 0.457 C_d \frac{A^*}{A_c}\Pi$	$\Pi = w\sqrt{\frac{2gh}{d^{3/2}T_0}}\left(d_{aw}^{\frac{7}{4}}\Delta T_{gw}^{\frac{1}{2}} + \Delta T_{aw}^{\frac{1}{2}}\left(d^{\frac{7}{4}} - d_{aw}^{\frac{7}{4}}\right)\right)$
Vertically linear, horizontally two semi-parabolic, transversely parabolic Eq. (38)	$V'''_{in,ltw} = 0.343 C_d \frac{A^*}{A_c}\Pi$	

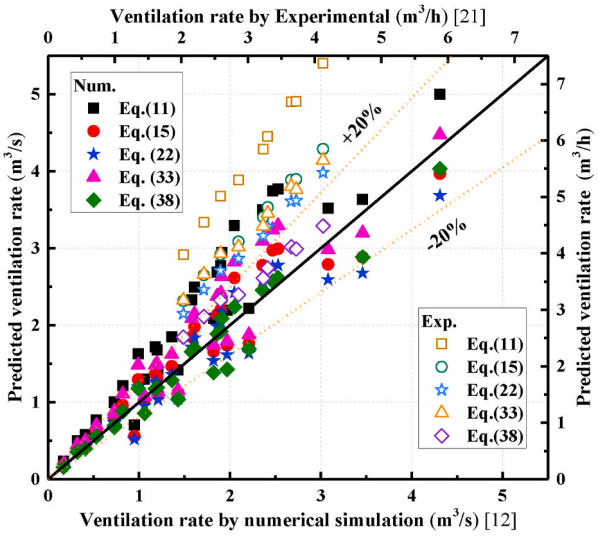

Fig. 3. Comparison of predictions by analytical model and previous results.

error of the predictions drops to 14.8 %. The average errors of prediction are much improved to 11.6 % under both vertically linear and horizontally semi-parabolic temperature distributions. For the two horizontal semi-parabolic temperature distributions in the depth direction, the average errors between numerical modelling and analytical models are 21.5 % and 11 % without and with consideration of the transversely parabolic temperature distribution in the width direction, respectively. The error of the analytical model considering the horizontally two semi-parabolic temperature distributions is influenced by the transmissivity and absorptivity of the glazing and the absorptivity of the absorber, which has not been considered in the numerical simulation and the other three analytical models. In this study, the transmissivity and absorptivity are selected on the basis of 3 mm glazing; this value may vary with different material usage.

Based on the above analysis, the predictions by Eq. (22) both considering the vertically linear and semi-parabolic temperature are close to the value calculated by Eq. (38) that considers the three-dimensional temperature distribution. However, the influence of material usage is not considered in Eq. (22). In other words, the radiation intensity inside the channel is considered to be the same as the external solar radiation intensity. This is contradictory to practical engineering. In summary, the established model of Eq. (38) considering the three-dimensional temperature distribution in this study can provide more accurate predictions for solar chimneys in tunnels.

4. Implementations

To implement the developed model in present study, a typical tunnel with dimensions of 240 m (length) × 10 m (width) × 5 m (height) is employed. The solar chimney is located in the middle of the tunnel ceiling. The solar intensity was selected as 800 W/m^2. Referring to the optimal values of cavity height 6 m [12]. It is difficult for structural safety that the solar chimney is installed across the whole tunnel. Thus, the effect of cavity height/width on ventilation rate are analyzed. Additionally, the impact of cavity height/depth, the absorptivity of the transparent glass is also analyzed.

Fig. 4 shows the volumetric flow rate under different cavity height/width. The vertically linear temperature significantly influences the ventilation rate. The effect of the transversely parabolic temperature distribution on the ventilation rate is more obvious than that of the horizontally semi-parabolic temperature distribution. It can be observed that the ventilation rate decreases with the cavity height/width. Therefore, extending the cavity width as far as possible can enhance the ventilation rate through the solar chimney because of the larger total

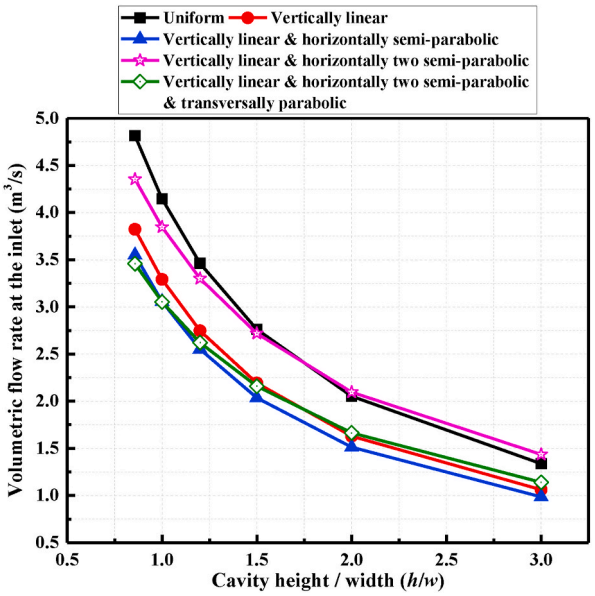

Fig. 4. Comparison of volumetric flow rate under different cavity height/width, d = 1.8m.

absorbed solar energy. Under different cavity height/width, the predictions by the analytical model considering the vertically linear and horizontally semi-parabolic temperatures are similar with the predictions by taking the 3D temperature profile into account but with more sluggish sensitivity.

Fig. 5 presents the volumetric flow rate under varied cavity height/depth. The airflow rate exponentially decreased along the ratio of cavity height to cavity depth. That means the ventilation performance improvement is insignificant during the cavity height/depth surpass 10, this is consistent with the optimum ratio for Trombe wall [16]. The predicted airflow rate based on the uniform temperature distribution and vertically linear & horizontally two piecewise semi-parabolic temperature profile is obviously higher than that value predicted by others model. The predictions calculated by Eq. (38) is lowest than other models.

Fig. 6 shows the volumetric flow rate at the inlet with different absorptivity of glazing. The ventilation rate is only varied with the absorptivity of glass by considering the horizontally two semi-parabolic temperature distributions, Eqs. (33) and (38). Thus, only the predictions using these two function are compared. The ventilation rate linearly

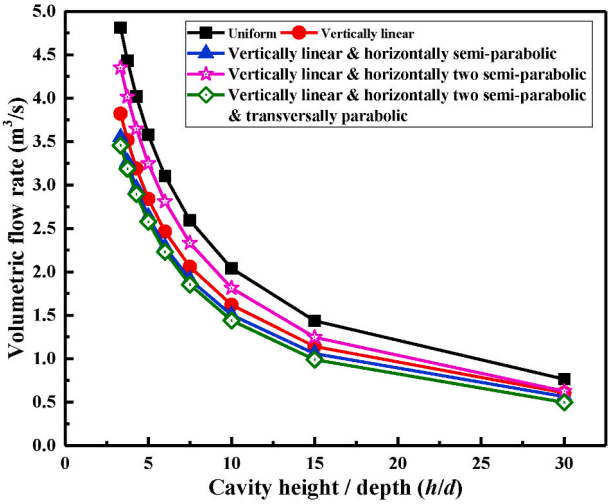

Fig. 5. Volumetric flow rate under different cavity height/depth, w = 7m.

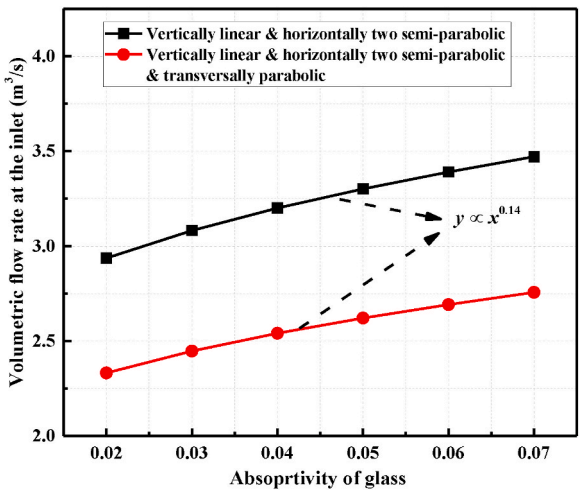

Fig. 6. Effect of absorptivity of glazing on ventilation rate.

increases with $\varepsilon^{0.14}$. The predictions by analytical model considering 3D temperature profile is less than that considering 2D temperature profile, that $V'''_{in,ltw} = 0.749V'''_{in,lts}$.

Based on the above analysis, the analytical model considering both the vertically linear and horizontally semi-parabolic temperature distribution (2D) and the analytical model considering the three-dimensional temperature distribution (3D) inside cavity are applied to obtain the ventilation rate through the solar chimney at the top of the tunnel. It is noteworthy that material usage was not taken into consideration in the analytical model, which considers vertically linear and horizontally semi-parabolic temperature distribution (2D). Therefore, the theoretical model of Eq. (38) considering the 3D temperature distribution may be the best choice for a solar chimney in a tunnel. This is due to the following reasons: (1) the temperature distribution is closer to the actual condition, (2) the effect of covered materials is considered, which can extend the application of the theoretical model, (3) the effect of tunnel and chimney configurations are both considered.

The established model in the present work provides technical guidance for the design of solar chimneys in tunnels that can improve the application of solar chimneys in tunnels. In tunnel applications, solar chimneys can enhance natural ventilation, thereby reducing the need for mechanical ventilation systems that consume electricity. This can significantly improve air quality inside tunnels by facilitating the removal of vehicle emissions and other pollutants, thus benefiting both the environment and human health. Moreover, a solar chimney can reduce the energy costs associated with tunnel operations. Over time, these savings can offset the initial investment costs and low maintenance costs compared with traditional mechanical ventilation systems.

5. Conclusions

Theoretical models were developed to predict the volumetric flow rate through a solar chimney in a tunnel. Five typical types of temperature distribution inside the chimney cavity are considered to propose the analytical models, as shown in Table 1. The following major conclusions can be made:

(1) The influence of the internal temperature distribution on the ventilation rate at solar chimney inlet is significantly, and the three-dimensional temperature distribution should be considered when evaluates the ventilation performance of the solar chimney. The covered material influences the ventilation rate significantly, which has been considered in the theoretical model based on the 3D temperature profile.

(2) The predictions by the analytical model considering both the vertically linear and horizontally semi-parabolic temperature distributions are close to the values calculated by the analytical model considering the three-dimensional temperature profile, while the average errors of prediction are 11.6 % and 11 % for the above two theoretical models.

(3) Considering two semi-parabolic temperature distributions in the cavity depth direction, the volumetric flow rate at the inlet is enhanced with smaller h/w and h/d, and that linearly increase with 0.14 power of the glazing absorptivity. The optimum ventilation performance through solar chimney in tunnel can be obtained with h/d equal to 10 and wider channel. The theoretical model considering the three-dimensional temperature distribution is the best choice for solar chimneys in tunnels.

In summary, this study provides an effective model for predicting the ventilation performance of solar chimneys and guides extraction design. The effect of external wind on solar chimney performance has been ignored to obtain an analytical solution that will be clearly explored in future work. Moreover, experiments of solar chimney applied in tunnel and the more validation will be done in our future research.

CRediT authorship contribution statement

Youbo Huang: Writing – original draft, Validation, Supervision, Project administration, Methodology, Funding acquisition, Formal analysis. **Bing Wang:** Writing – original draft, Investigation, Formal analysis. **Chengjia Luo:** Software, Data curation. **Long Shi:** Writing – review & editing, Software, Methodology. **Ning Lu:** Writing – review & editing, Supervision, Resources, Conceptualization. **Bingyan Dong:** Writing – original draft. **Hua Zhong:** Writing – review & editing, Data curation.

Declaration of competing interest

The authors declare that they have no known competing financial interests or personal relationships that could have appeared to influence the work reported in this paper.

Acknowledgments

The authors acknowledge support from the Natural Science Foundation of Chongqing, China [Grant No. CSTB2024NSCQ-MSX1210], National Natural Science Foundation of China (NSFC) [Grant No. 52104185, 52274235], the Science and Technology Research Program of Chongqing Municipal Education Commission [Grant No. KJQN202101527], Opening Fund of State Key Laboratory of Fire Science (HZ2023-KF07).

References

[1] J.O. Aguilar, J. Xaman, G. Álvarez, I. Hernández-Pérez, C. López-Mata, Thermal performance of a double pane window using glazing available on the Mexican market, Renew. Energy 81 (2015) 785–794, https://doi.org/10.1016/j.renene.2015.03.063.

[2] Y. Tao, X. Fang, M.Y.L. Chew, L. Zhang, J. Tu, L. Shi, Predicting airflow in naturally ventilated double-skin facades: theoretical analysis and modelling, Renew. Energy 179 (2021) 1940–1954, https://doi.org/10.1016/j.renene.2021.07.135.

[3] T.H. Long, N.J. Zhao, W.Y. Li, S. Wei, Y.C. Li, J. Lu, S. Huang, Z.Y. Qiao, Natural ventilation performance of solar chimney with and without earth-air heat exchanger during transition seasons, Energy 250 (2022) 123818, https://doi.org/10.1016/j.energy.2022.123818.

[4] N. Monghasemi, A. Vadiee, A review of solar chimney integrated systems for space heating and cooling application, Renew. Sustain. Energy Rev. 81 (2018) 2714–2730, https://doi.org/10.1016/j.rser.2017.06.078.

[5] J. Kong, J. Niu, C. Lei, A CFD based approach for determining the optimum inclination angle of a roof-top solar chimney for building ventilation, Sol. Energy 198 (2020) 555–569, https://doi.org/10.1016/j.solener.2020.01.017.

[6] L. Shi, G. Zhang, W. Yang, D. Huang, X. Cheng, S. Setunge, Determining the influencing factors on the performance of solar chimney in buildings, Renew.

Sustain. Energy Rev. 88 (2018) 223–238, https://doi.org/10.1016/j.rser.2018.02.033.
[7] K.S. Ong, A mathematical model of a solar chimney, Renew. Energy 28 (2003) 1047–1060, https://doi.org/10.1016/S0960-1481(02)00057-5.
[8] K.S. Ong, C.C. Chow, Performance of a solar chimney, Sol. Energy 74 (2003) 1–17, https://doi.org/10.1016/S0038-092X(03)00114-2.
[9] K.T. Andersen, Theory for natural ventilation by thermal buoyancy in one zone with uniform temperature, Build. Environ. 38 (2003) 1281–1289, https://doi.org/10.1016/S0360-1323(03)00132-X.
[10] L. Shi, Theoretical models for wall solar chimney under cooling and heating modes considering room configuration, Energy 165 (2018) 925–938, https://doi.org/10.1016/j.energy.2018.10.037.
[11] L. Shi, G. Zhang, An empirical model to predict the performance of typical solar chimneys considering both room and cavity configurations, Build. Environ. 103 (2016) 250–261, https://doi.org/10.1016/j.buildenv.2016.04.024.
[12] X.D. Cheng, Z.C. Shi, K. Nguyen, L.H. Zhang, Y. Zhou, G.M. Zhang, J.H. Wang, L. Shi, Solar chimney in tunnel considering energy-saving and fi re safety, Energy 210 (2020) 118601, https://doi.org/10.1016/j.energy.2020.118601.
[13] A. Sengupta, D.P. Mishra, S.K. Sarangi, Computational performance analysis of a solar chimney using surface modifications of the absorber plate, Renew. Energy 185 (2022) 1095–1109, https://doi.org/10.1016/j.renene.2021.12.089.
[14] H. Wang, C. Lei, A numerical investigation of combined solar chimney and water wall for building ventilation and thermal comfort, Build. Environ. 171 (2020) 106616, https://doi.org/10.1016/j.buildenv.2019.106616.
[15] G. He, D. Lv, Distributed heat absorption in a solar chimney to enhance ventilation, Sol. Energy 238 (2022) 315–326, https://doi.org/10.1016/j.solener.2022.04.047.
[16] L. Shi, G. Zhang, X. Cheng, Y. Guo, J. Wang, M.Y.L. Chew, Developing an empirical model for roof solar chimney based on experimental data from various test rigs, Build. Environ. 110 (2016) 115–128, https://doi.org/10.1016/j.buildenv.2016.10.002.
[17] K.E. Amori, S.W. Mohammed, Experimental and numerical studies of solar chimney for natural ventilation in Iraq, Energy Build. 47 (2012) 450–457, https://doi.org/10.1016/j.enbuild.2011.12.014.
[18] Q. Wang, G. Zhang, Q. Wu, L. Shi, Solar chimney performance in buildings under three heating modes: an empirical analysis, Sustain. Energy Technol. Assessments 52 (2022) 102222, https://doi.org/10.1016/j.seta.2022.102222.
[19] M.A. Leon, S. Kumar, Mathematical modeling and thermal performance analysis of unglazed transpired solar collectors, Sol. Energy 81 (2007) 62–75, https://doi.org/10.1016/j.solener.2006.06.017.
[20] Q. Wang, G. Zhang, W. Li, L. Shi, External wind on the optimum designing parameters of a wall solar chimney in building, Sustain. Energy Technol. Assessments 42 (2020) 100842, https://doi.org/10.1016/j.seta.2020.100842.
[21] Y.B. Huang, X. Liu, L. Shi, B.Y. Dong, H. Zhong, Enhancing solar chimney performance in urban tunnels: investigating the impact factors through experimental and theoretical model analysis, Energy 282 (2023) 128329, https://doi.org/10.1016/j.energy.2023.128329.
[22] L. De Oliveira, F. Marques, Aerodynamics Simulation and measurements of wind interference on a solar chimney performance, J. Wind Eng. Ind. Aerod. 179 (2018) 135–145, https://doi.org/10.1016/j.jweia.2018.05.020.
[23] L. Shi, Impacts of wind on solar chimney performance in a building, Energy 185 (2019) 55–67, https://doi.org/10.1016/j.energy.2019.07.056.
[24] Y.D. Wang, P.X. Du, Y.Y. Chen, S.H. Hua, J. Wang, C. Shi, K. Liu, Mixed ventilation approach combined with single-shaft complementary system for Highway tunnels, Tunn. Undergr. Space Technol. 132 (2023) 104927, https://doi.org/10.1016/j.tust.2022.104927.
[25] S.A.M. Burek, A. Habeb, Air flow and thermal efficiency characteristics in solar chimneys and Trombe Walls, Energy Build. 39 (2007) 128–135, https://doi.org/10.1016/j.enbuild.2006.04.015.
[26] S. Suhendri, M. Hu, Y. Su, J. Darkwa, S. Riffat, Performance evaluation of combined solar chimney and radiative cooling ventilation, Build. Environ. 209 (2022) 108686, https://doi.org/10.1016/j.buildenv.2021.108686.
[27] T.Y. Long, Z.P. Cai, Fluid Mechanical, China Architecture & Building Press, China, 2019.